

Light scattering efficiency of dielectric spheres

CHATAR SINGH, R.N. SINGH

Physics Department, Indian Institute of Technology, Delhi, Hauz Khas, New Delhi-110016, India.

A theoretical study of individual and collective contributions of electric and magnetic multipoles to light scattering efficiency of dielectric spheres is presented.

1. Introduction

A rigorous solution of the problem of scattering of a plane monochromatic electromagnetic wave due to a sphere given by Mie and Debye [1] leads to the following expression for Q_{sca} , dimensionless normalized scattering efficiency:

$$Q_{\text{sca}} = \frac{2}{\alpha^2} \sum_{n=1}^{\infty} (2n+1) [|a_n|^2 + |b_n|^2], \quad (1)$$

where α is the dimensionless particle size parameter equal to $\pi D/\lambda$, D being the diameter of the sphere, a_n and b_n are Mie scattering coefficients, both of which are the functions of complex refractive index μ of the particle. In fact, a scattered radiation is a superposition of electric and magnetic multipole radiations, while a_n and b_n are the respective multipole moments [1]. It is well known that the curves of Q_{sca} with α show smooth variation superimposed by ripple structure. MEVEL [2], METZ and DETMAR [3] and CHYLEK [4, 5] have related, in a detailed way, the ripple structure to the properties of Mie scattering coefficients. In this paper, an attempt has been made to study the individual and cumulative effects of contribution of electric and magnetic multipoles to the scattering efficiency. This work is a part of the ongoing program of research work on light scattering by aerosols, the measurement being done at the Physics Department, Indian Institute of Technology, Delhi.

2. Theory

The scattering efficiency factor Q_{sca} given by (1) may also be written as

$$\begin{aligned} Q_{\text{sca}} &= \frac{2}{\alpha^2} \sum_{n=1}^{\infty} (2n+1) |a_n|^2 + \frac{2}{\alpha^2} \sum_{n=1}^{\infty} (2n+1) |b_n|^2 \\ &= \sum_{n=1}^{\infty} q_e^n + \sum_{n=1}^{\infty} q_m^n = C_{\text{em}} + C_{\text{mm}}, \end{aligned} \quad (2)$$

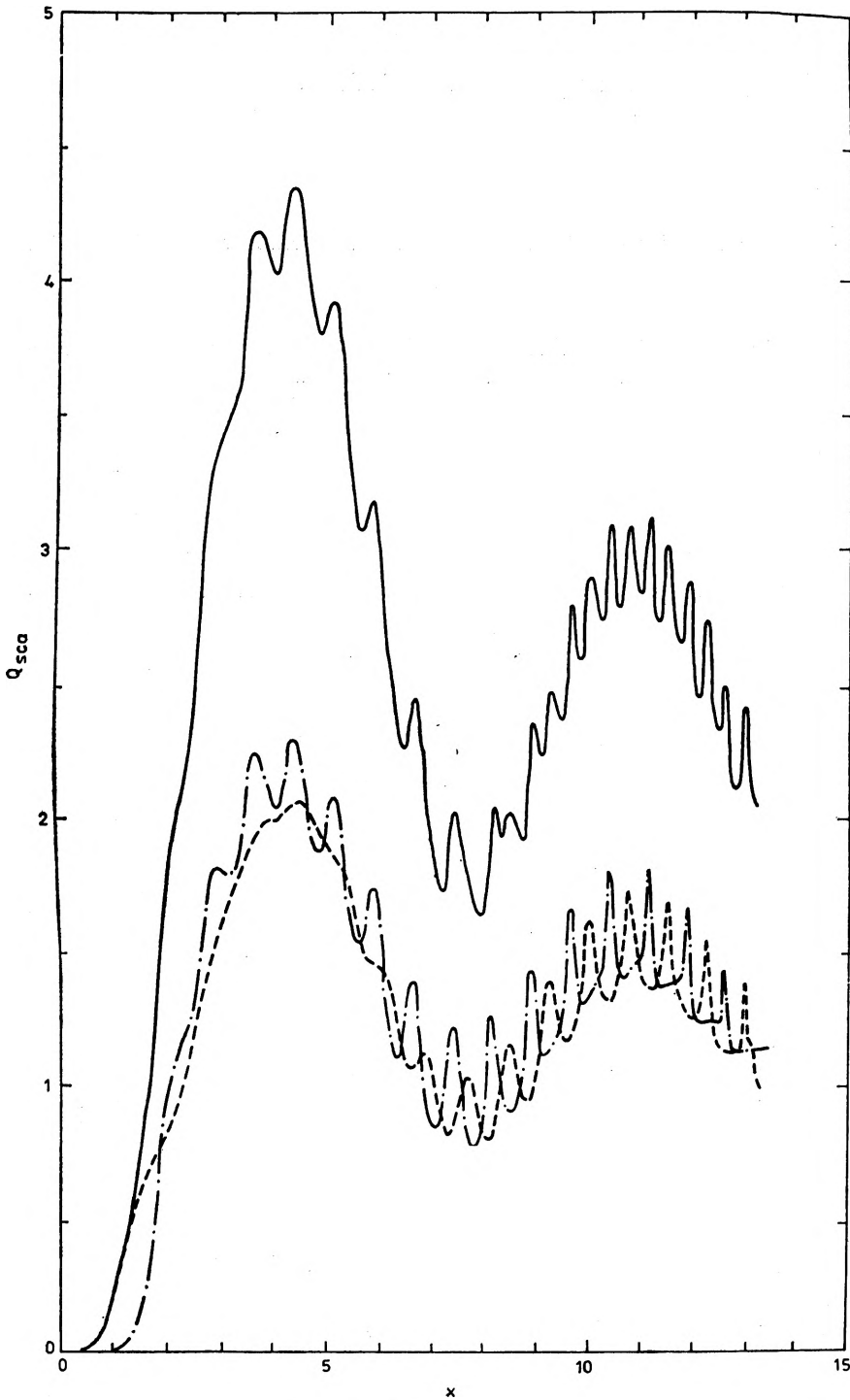


Fig. 1. Q_{sca} , C_{em} and C_{mm} for $\mu = 1.5$ plotted against x to compare the contributions of C_{em} and C_{mm} to scattering efficiency Q_{sca} (refractive index = 1.5; — Q_{sca} , -.-.- C_{mm} , - - - C_{em})

where q_e^n and q_m^n represent the contribution of n -th electric and magnetic multipole: and C_{em} and C_{mm} represent the contribution of all the electric and magnetic multipoles, respectively. A program for computer ICL 2960 was written to calculate Q_{sca} , q_e^n , q_m^n , C_{em} and C_{mm} . a was varied up to 15, by 0.01 steps for the following values of $\mu = 1.33, 1.45, 1.50, 1.60, 1.70, 2.0, 1.5-10.001, 1.5-10.01,$ and $1.5-10.1$. Q_{sca} , C_{em} , C_{mm} , q_e^n and q_m^n were plotted for $a \leq 15$ for real refractive indices out the above values of μ .

3. Results and discussion

3.1. Variation of C_{em} and C_{mm} with a

Figure 1 shows the variations of Q_{sca} , C_{em} and C_{mm} with a . From all these curves the following observations can be made.

To each peak in C_{em} and C_{mm} curves there corresponds a peak in Q_{sca} curve which shows that the resonance peaks in Q_{sca} curve are caused by the resonance structure in C_{em} and C_{mm} curves.

For $2 \leq a \leq 6$ these curves have practically no resonance peaks in C_{em} curve. Thus, for $2 \leq a \leq 6$ only resonance peaks due to magnetic multipoles are visible in the Q_{sca} curve. Therefore, it may be inferred that in this region the light

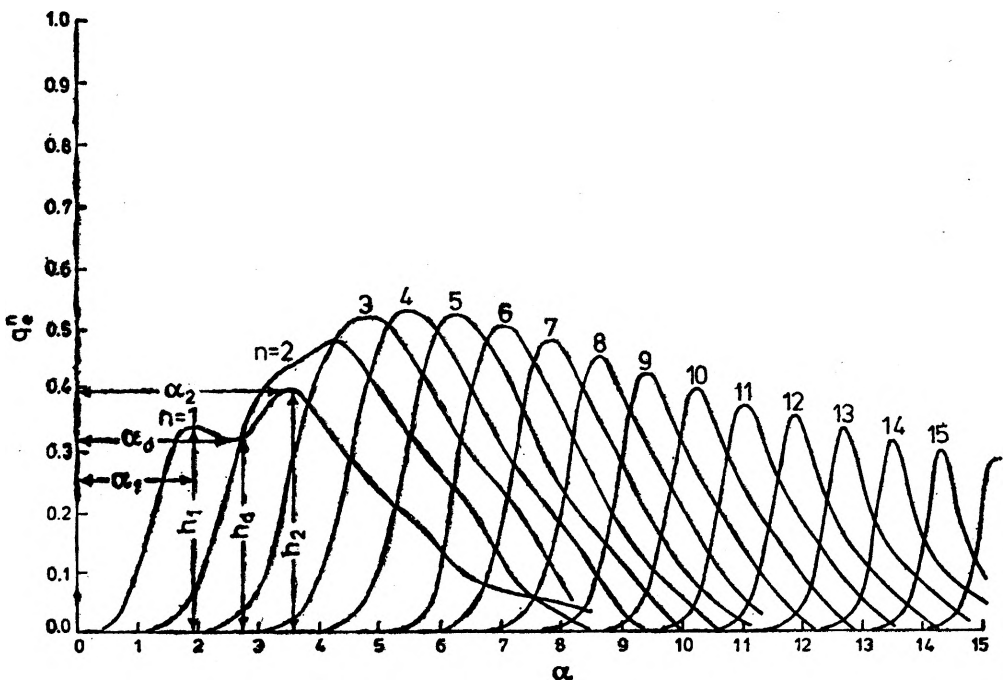


Fig. 2. Contribution of the electric multipoles to the scattering efficiency q_e^n for $\mu = 1.33$, plotted against a (refractive index - 1.33)

is scattered more strongly by magnetic multipoles than by electric multipoles. The sharpness of all the resonance peaks increases.

An increase in μ results in a compression of all the three Q_{sca} , C_{em} , and C_{mm} curves towards the origin and the peaks become more and more sharp.

3.2. Variation of q_e^n and q_m^n with a

These curves were plotted earlier by MEVEL [2], and METZ and DETTMAR [3] for all the values of μ mentioned in Section 2, only for $\mu \geq 2$; that is why some observations seem to have been missed. Figures 2 and 3 show the q_e^n and q_m^n curves, respectively, for $\mu = 1.33$. From similar curves plotted for $1.33 \leq \mu \leq 2$, the following observations can be made.

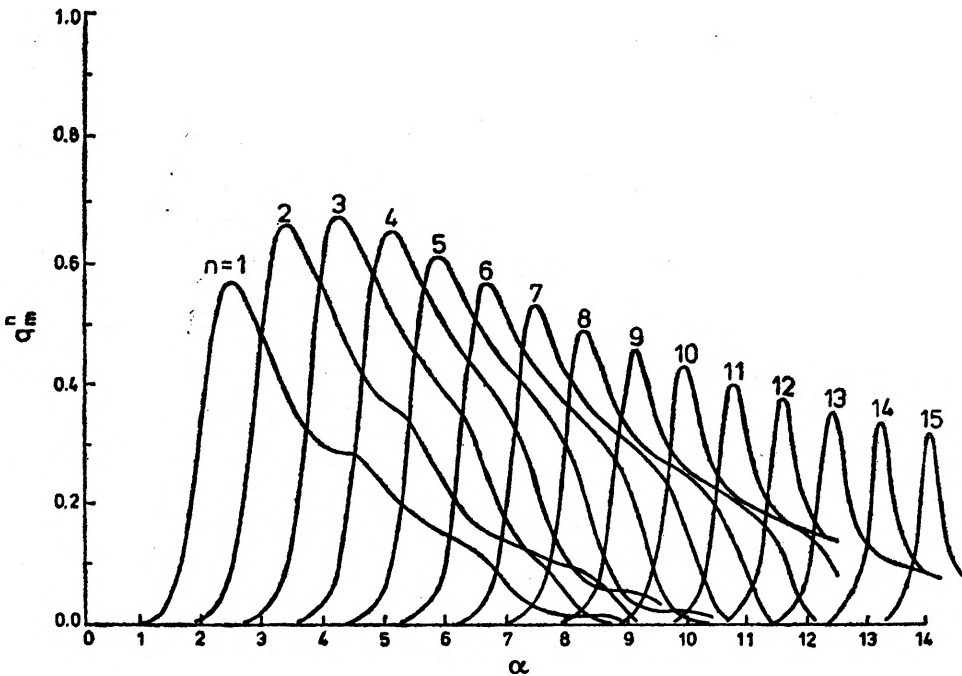


Fig. 3. Contribution of the magnetic multipoles to the scattering efficiency, q_m^n for $\mu = 1.33$, plotted against a (refractive index - 1.33)

A comparison of Figs. 1-3 shows that it is only electric dipole (q_e^n with $n = 1$) which mainly contributes to Q_{sca} for $a \leq 1$ and $1.33 \leq \mu \leq 2.0$. It may also be seen that as μ decreases the electric dipole contribution dominates for higher values of a .

For different values of n the peak values of q_e^n and q_m^n curves at first rise slightly then, they fall. The peak values of q_e^n and q_m^n curves and each value of n have been plotted for different values of real refractive indices (Fig. 4). It

is noticed that as μ is of the order of 1.7, the peak contribution only decreases instead of being first rised. However, for all the values of μ and n peak contribution of magnetic multipoles is higher that that of electric multipoles. It is also seen from Fig. 4 that the difference in peak contribution of q_m^n and q_e^n for

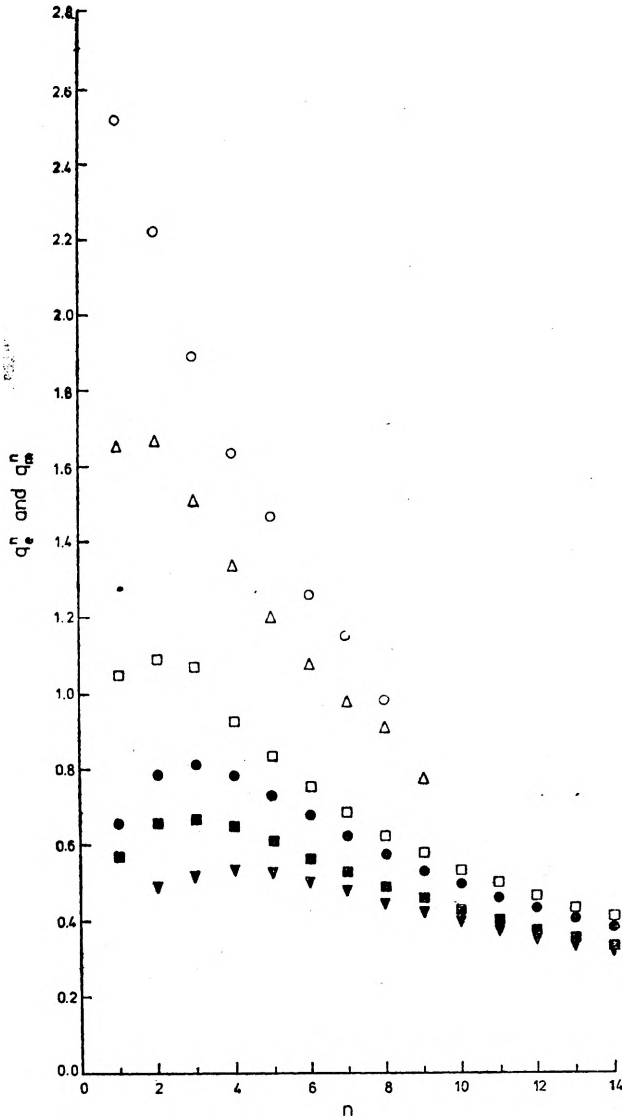


Fig. 4. Peak values of q_e^n and q_m^n plotted against n , for $\mu = 1.33, 1.5$ and 2.0 ($\circ - q_m^n, m = 2.00$; $\triangle q_e^n, m = 2.00$; $\square q_m^n, m = 1.50$; $\bullet q_e^n, m = 1.50$; $\blacksquare q_m^n, m = 1.33$; $\blacktriangledown q_e^n, m = 1.33$)

the some value of n is greater for low values of n , except for the first few values. This difference becomes very small for higher values of n . In fact, for all the values of μ this difference remains constant for $n \geq 8$.

As n increases each of q_e^n and q_m^n peaks becomes sharper. This is seen clearly in Fig. 5 which shows a full width at half maximum (FWHM) of each peak, plotted against n for different values of μ . For $\mu > 1.5$ FWHM falls as n increases.

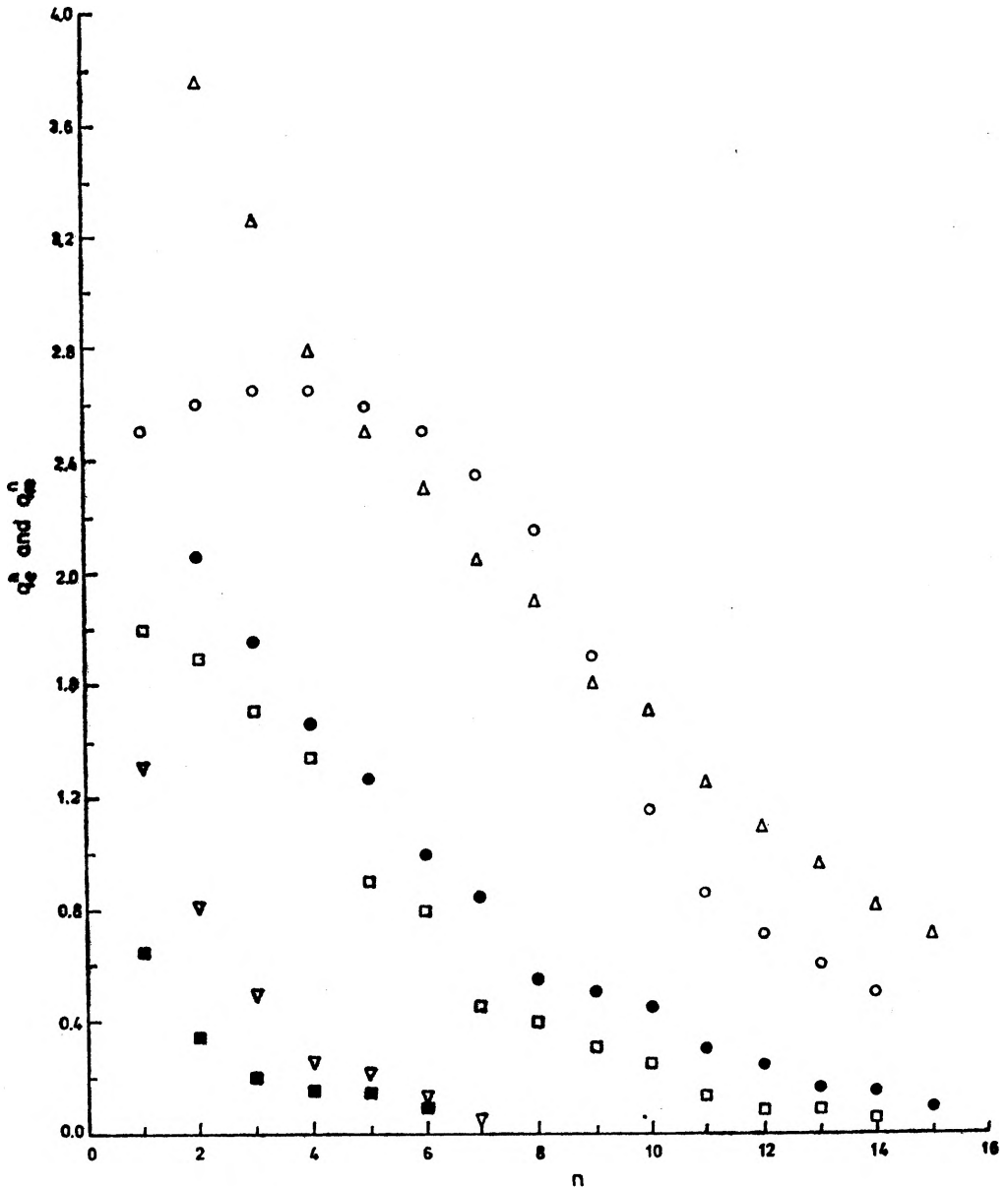


Fig. 5. FWHM of q_e^n and q_m^n peaks plotted against n , for $\mu = 1.33, 1.5$ and 2.0 (● $q_e^n, m = 1.50$; □ $q_m^n, m = 1.50$; △ $q_e^n, m = 1.33$; ○ $q_m^n, m = 1.33$; ▽ $q_e^n, m = 2.00$; ■ $q_m^n, m = 2.00$)

For $\mu < 1.5$ FWHM falls only for electric multipoles. For magnetic multipoles it first rises slightly for few values of n and then falls. It may also be seen that, except for $\mu < 1.5$, FWHM is greater for electric multipoles than for magnetic multipoles.

The variation of q_e^n with a , for different values of μ and $n = 1$, shows (Fig. 2) a double peak structure for $\mu \leq 1.7$ (approx.) The double peak behaviour is not seen for the values of $\mu \geq 1.7$ (Fig. 6).

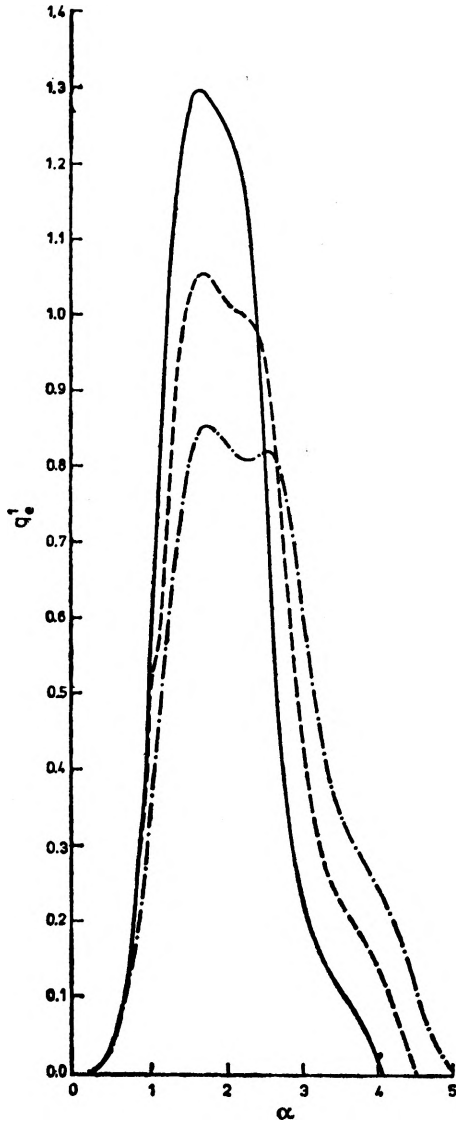


Fig. 6. q_e^1 plotted against a for $\mu = 1.6$, 1.7, and 1.82 (— $m = 1.82$, - - - $m = 1.7$, - . - . - $m = 1.6$)

Figure 7 shows the variations in the positions of first peak (a_1), second peaks (a_2) and the dip (a_d) in the q_e^1 curves plotted against a occurring with the increase of μ . It may be seen that the difference in a_1 and a_d remains nearly the same but approaches a_2 very rapidly. Variation of $\Delta a = a_2 - a_1$ is also shown in the same figure and it may be noted that Δa falls nearly linearly with μ .

Figure 8 shows variations of the heights of the first and second peaks h_1 , h_2 and the height of the dip h_d , in the curve q_e^1 against a (Fig. 2). It may be observed that: i) h_1 and h_2 increase linearly with μ , ii) h_1 increases faster than h_2 , iii) for $\mu = 1.5$, $h_1 = h_2$, and iv) h_d rises almost linearly with μ .

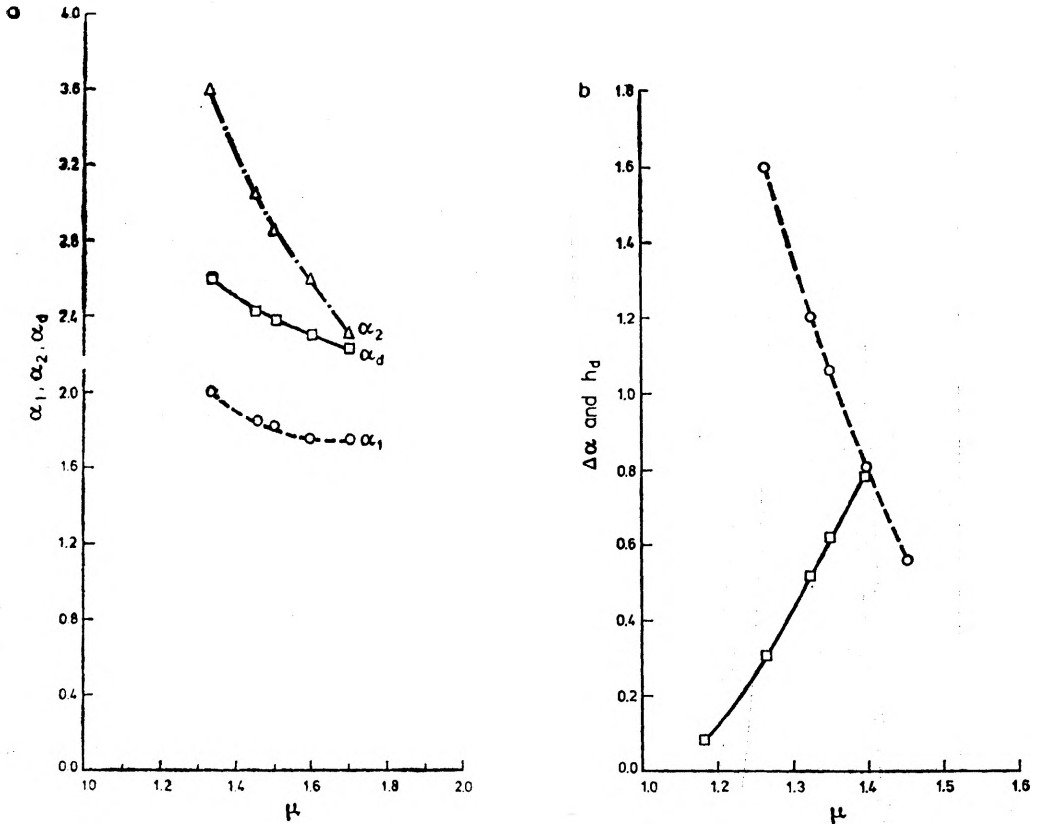


Fig. 7. Peak values α_1 and α_2 of two peaks, α_d , value of dip, in q_e^1 curve, plotted against μ (a); $\Delta\alpha$ and h_d plotted against μ : ($\circ - - - \circ$ ($\alpha_2 - \alpha_1$) = $\Delta\alpha$, $\square - \square$ h_d) (b)

If α_m^n and α_e^n denote the values of a for which there occur n -th peaks in q_m^n and q_e^n curves, respectively, a variation of α_m^n and α_e^n (Fig. 9) with n , for different values of μ , shows that: i) $\alpha_e^n > \alpha_m^n$, which means that the peak due to n -th electric multipole occurs for a greater value of a than the peak due to n -th magnetic multipole, ii) the difference $(\alpha_e^n - \alpha_m^n)$ is constant except for $n < 4$. This shows that separation of resonance structure due to n -th electric and magnetic multipoles remains constant as a increases, iii) the difference $(\alpha_e^{n+1} - \alpha_e^n)$ or $(\alpha_m^{n+1} - \alpha_m^n)$ is the same for all the values of $n \geq 4$, but is different for different values of μ . A close observation of q_e^n and q_m^n curves (Figs. 2 and 3) shows a slight flattening of peaks, near the base, towards higher value of a .

q_e^1 curves against a were plotted for $1.16 \leq \mu \leq 2$. The behaviour of q_e^1 curve, as seen above, shows that probably each of q_e^n and q_m^n curves exhibits a double peak structure even for $n > 1$, though the second peak is not at all relatively strong and hence the flattening near the base.

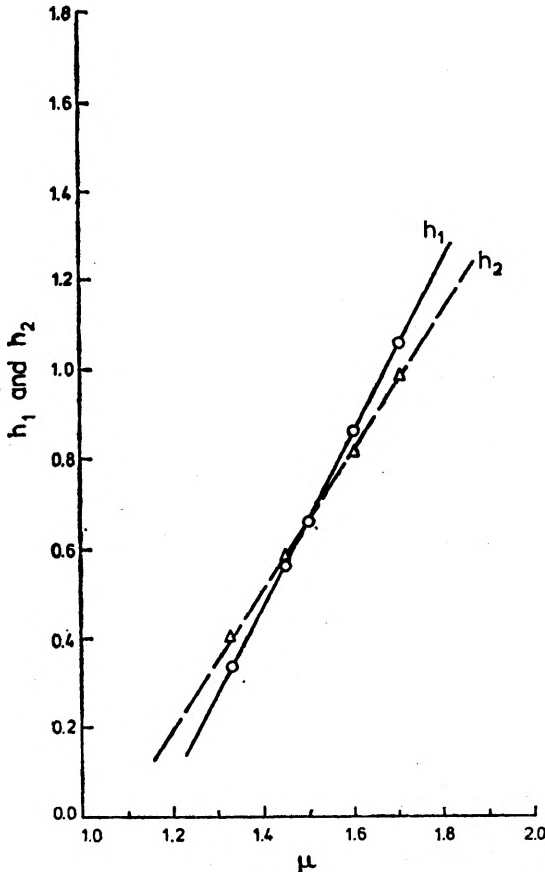


Fig. 8. Heights h_1 and h_2 of two peaks in q_e^1 curves, plotted against μ

Figure 10 shows the variation of q_m^1 curve with a for $\mu = 1.16$. This curve shows also a double peak structure which however, is not observed for $\mu > 1.33$ (cf. Figs. 2 and 3).

Figure 11 shows a plot of q_m^{10} and q_m^{12} against a for $\mu = 1.5$. It can be noticed that q_m^{10} and q_m^{12} show low secondary peaks which contribute to the broad variations in Q_{sca} with a curve for higher values of a .

3.3. Complex refractive indices

Some similar curves were plotted for complex refractive indices $\mu = 1.5-10.001$, $1.5-10.01$, and $1.5-10.1$. It is seen that: i) the nature of all the curves remains the same, ii) the curves become more smooth and lower as the imaginary part of the refractive index increases, iii) the values of a_1 and a_2 remain the same as those for the real part of the complex refractive index, but h_1 and h_2 decrease.

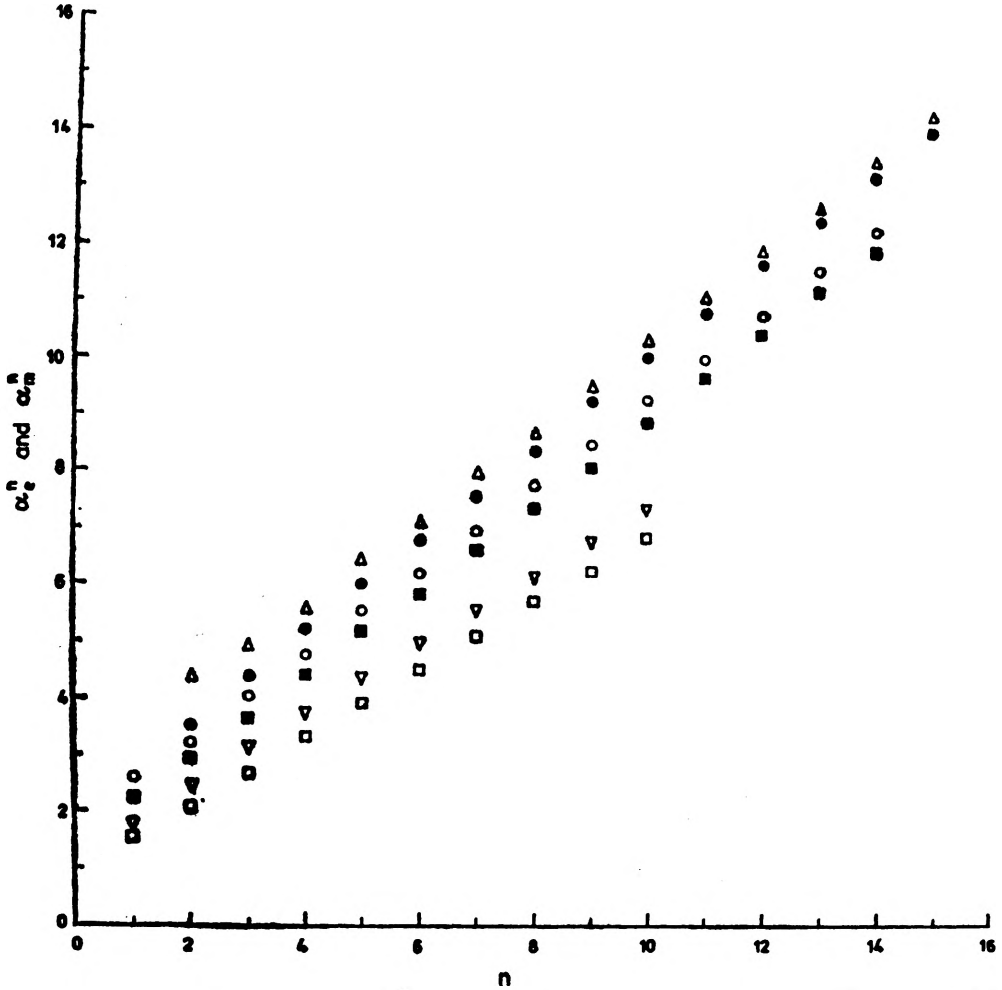


Fig. 9. α_m^n and α_c^n plotted against n , for $\mu = 1.33, 1.5$ and 2.0 ($\Delta \alpha_c^n, m = 1.33$; $\bullet \alpha_m^n, m = 1.33$; $\circ \alpha_c^n, m = 1.50$; $\blacksquare \alpha_m^n, m = 1.50$; $\nabla \alpha_c^n, m = 2.00$; $\square \alpha_m^n, m = 2.00$)

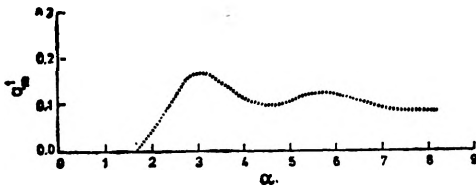


Fig. 10. Contribution of the magnetic dipole q'_m plotted against α , for $\mu = 1.16$

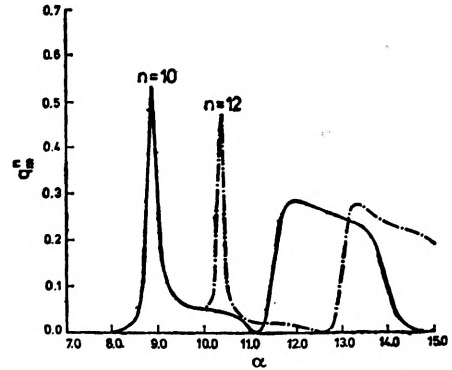


Fig. 11. Contribution of the 10-th and 12-th magnetic multipoles q_m^{10} and q_m^{12} to Q_{scat} plotted against α , for $\mu = 1.5$

4. Concluding remarks

These calculations have been performed only up to $a = 15$. It might be an interesting idea to extend these calculations for higher values of a . The effect of changing real part of the complex refractive index has not been studied either. It is hoped that these observations will help to better understand the light scattering by aerosols and resonance structure in scattering efficiency parameters. Work is already progressing in our group, in this direction.

Acknowledgements—Some useful discussions with Prof. Nath, Prof. P.K.C. Pillai and Dr. S.K. Chattopadhyaya are thankfully acknowledged.

References

- [1] KERKER M., *The Scattering of Light and other Electromagnetic Radiations*, Academic Press, New York 1969.
- [2] MEVEL J., Ref. [1], p. 115.
- [3] METZ H., DETTMAR J., Ref. [1], p. 116.
- [4] CHYLEK P., *J. Opt. Am.* **66** (1976), 285.
- [5] CHYLEK P., KIEHL J.T., KO M.K.W., *Phys. Rev.* **A18** (1978), 2229.

Received August 19, 1981

Эффективность рассеяния света на диэлектрических сферах

Описаны теоретические исследования индивидуальных и коллективных разработок к вопросу об электрических и магнитных мультиполях относительно эффективности рассеяния света на диэлектрических сферах.